



## COBEM-2021-1185

# THE FORMATION OF NITRIC OXIDE IN FLAMES: A NUMERICAL ASSESSMENT USING DETAILED CHEMICAL KINETICS

### Vinicius Rugeri Borges Bonini

vinicius.bonini@lepten.ufsc.br

Laboratory of Energy Conversion Engineering and Energy Technology - Technological Center - Federal University of Santa Catarina - LEPTEN/CTC/UFSC.

Trindade, Florianópolis, SC, CEP 88040-900, Brazil.

### Moisés Abreu de Sousa

moissousa@unifesspa.edu.br

Department of Mechanical Engineering - Federal University of South and Southeast of Pará - UNIFESSPA

### Kathleen Mayara Balestrin

kmbalestrin@labcet.ufsc.br

### Jônatas Vicente

jonatas.vicente@labcet.ufsc.br

Combustion and Thermal Systems Engineering Laboratory - Mechanical Engineering - Federal University of Santa Catarina - LABCET/EMC/CTC/UFSC..

Trindade, Florianópolis, SC, CEP 88040-900, Brazil.

### Leonel R. Cancino

leonel.cancino@labmci.ufsc.br

Internal Combustion Engines Laboratory - Joinville Technological Center - Federal University of Santa Catarina - LABMCI/CTJ/UFSC. Rua Dona Francisca 8300, Joinville, SC, Brazil, CEP 89219-600

**Abstract.** Nitric oxide emissions derived from the combustion process, is a topic of great concern due to the environmental impact caused by this pollutant. In this sense, there is a demand to understand how these chemical compounds are formed in the course of combustion. Numerically, the chemical kinetics of a combustion process can be represented by kinetics models in which a set of chemical reactions describes the kinetics evolution of chemical species along the combustion process. Regarding the formation of  $NO_x$  compounds, it occurs through five known routes, which depend on the thermochemical conditions of the mixture. In this work, experimental  $NO_x$ -related data (in the post-flame region) available in the literature was collected and used for validation of detailed kinetics models also available in the literature. It was identified that there are some disagreements between the results calculated by different models and the experimental data of the literature. Multicomponent transport, thermal diffusion, and radiative heat losses were left into account for the calculations in the CANTERA software. The detailed kinetics models were compared in terms of the  $NO$  mole fraction in the post-flame products, laminar burning velocity, and it was verified that the model proposed by Capriolo has the best agreement with the experimental data.

**Keywords:** Nitric oxide, Detailed chemical kinetics models, CANTERA Software.

## 1. INTRODUCTION

In 2019, the global primary energy was 602.27 EJ, of which, 31% (188.91 EJ) were supplied by oil, 26% (157.51 EJ) were by coal and 23% (139.00 EJ) were by natural gas. On the other hand, the renewable sources contributed with 14%, showing a growth of 12.2% between 2018 and 2019 (IEA, 2019). It is clear that the combustion of fossil fuels is the primary source of energy generation worldwide, especially for industrial processes (Ali *et al.*, 2020).

Among the types of equipment that are driven by fossil fuels, must be highlighted the internal combustion engines (ICE), these kinds of engines are massively employed in vehicles, small electricity power generators, and many other mechanical equipments. The internal combustion engines are mostly fueled by fossil fuels, such as gasoline and diesel, however, due to the constantly fluctuating prices of crude oil and the depletion of its reserves, happened an increasing interest in the search for alternative fuels, more specific the biofuels (Lubrano Lavadera *et al.*, 2021).

Besides the enormous use of fossil fuels, this type of fuels produce some pollutants, such as  $SO_x$  and  $NO_x$ , that

results in acid rain and photochemical smog (Ali *et al.*, 2020). The emissions of nitric oxides ( $NO_X$ ), from the combustion processes, are a topic of great concern, due to their environmental impact and also the more and more stringent regulations on pollutant emissions. In this manner, many researchers focused on the investigation of the underlying chemistry, searching to understand how these pollutants are formed (Watson *et al.*, 2016; Maroa and Inambao, 2020; Han *et al.*, 2021; Lubrano Lavadera *et al.*, 2021).

The  $NO_X$  emissions are composed of  $NO$  and  $NO_2$ , but mainly of  $NO$  (Maroa and Inambao, 2020). In this sense, the comprehension of the combustion chemistry of the  $NO$  formation in internal engines and other processes through experimental data and the development of accurate kinetic models is an important next step for the design of clean combustion engines (Capriolo *et al.*, 2021).

In this sense, the work made by Watson *et al.* (2016) analyzed the influence of  $C_1 - C_3$  alkane and alcohols structures on the formation of  $NO$  in premixed stagnation flames at atmospheric pressure. The results show that the alkane produces more  $NO$  than the alcohols, with this behavior being explained by the tendency of the alcohols to produce a lower concentration of the  $CH$  radical, and the lower flame temperature of alcohol flames, with his phenomena being considered in the thermochemical models available.

McCaffery *et al.* (2021) measured the  $NO_X$  emissions from 50 heavy-duty vehicles with different engine technologies and features on California roadways, employing the portable emissions measurement system (PEMS). The emissions testing was done in refuse haulers, school and transit buses, delivery vehicles, and goods movement vehicles, while they were operating in their normal routes in the South Coast Air Basin. The authors point out that the diesel vehicles generally got higher brake-specific  $NO_X$  emissions compared to the compressed natural gas (CNG) vehicles, with the  $NO_X$  emissions being strongly dependent on the selective catalytic reduction temperature (SCR). The diesel hybrid electric vehicles showed important  $NO_X$  benefits when compared to the conventional diesel vehicles, but higher emissions compared to the CNG and LPG (liquified petroleum gas) vehicles. The authors concluded that the reduction in  $NO_X$  emission was more pronounced for the CNG engines, the diesel hybrid electric, and LPG vehicles, compared to the diesel vehicles, indicating, that the advanced technologies and alternative fuels may provide important  $NO_X$  reductions.

Orooji *et al.* (2021) made a numerical and experimental analysis of the effects of injecting natural gas on  $NO_X$  re-burning by  $CO$  and  $CH$  radicals at the rotary cement kiln exhaust, as long as the thermal  $NO_X$  is very high in the rotary cement kiln. The results obtained in the article, show that can be reached an  $NO_X$  reduction from 30% to 70%. The results prove that the  $NO_X$  return in the swirling region is increased and  $NO_X$  concentration reduced.

In this sense, the main objective of this paper is to assess the formation of nitric oxide in flames using detailed chemical kinetics mechanisms. The prediction of the  $NO$  molar fractions, the laminar burning velocity, and the temperature in the post-flame region are going to be compared to experimental data found in the literature in order to determine the agreement between the model and the data.

## 2. LITERATURE REVIEW

The present paper focuses on the understanding of the prediction of the  $NO_X$  fractions in the post-flame region through combustion simulation using detailed kinetics mechanisms, therefore, the main topics referred to the  $NO_X$  routes formation and the kinetics models are going to be presented. Concerning the  $NO_X$ , the five known routes are presented with the main information of each of them. Regarding the kinetics mechanisms, the most recent mechanisms developed are presented.

### 2.1 $NO_X$ Routes

The five known  $NO_X$  formation routes are the thermal route, the prompt route, the  $N_2O$  route, the  $NNH$  route, and the  $N$  from the fuel. The routes are going to be briefly explained in the following subsections.

#### 2.1.1 Thermal route

The thermal  $NO$  route comes from the oxidation of nitrogen in the air at high temperatures, being the dominant source of  $NO$  at high temperatures and long residence times (Martins and Ferreira, 2010). The set of chemical reactions that describes this mechanism were proposed by Zeldovich, and are:



Zeldovich concluded that the formation of  $NO$  is much slower than the rate of combustion reactions and, that most of the  $NO$  fraction is formed after the complete combustion. Therefore, the thermal  $NO$  formation process could be decoupled from the combustion process and its formation rate calculated assuming equilibrium of the reactions of combustion (Martins and Ferreira, 2010).

### 2.1.2 Immediate formation route

The formation of  $NO$  through the prompt route occurs faster than the thermal  $NO$ . After Zeldovich, Fenimore observed that the  $NO$  formation rate at the flame front exceeded the predicted by the thermal route in fuel rich mixtures close to stoichiometry. The immediate  $NO$  formation mechanism can be broken down into fuel-poor and fuel-rich conditions. Since the  $CH$  concentration decreases under excess air conditions, immediate  $NO$  is very important under stoichiometric and fuel-rich conditions (De Soete, 1975; Martins and Ferreira, 2010). The most important initiation step is Reaction 4, and also the reaction Reaction 5 that contributes to break  $N_2$  in high temperatures.



### 2.1.3 $N_2O$ -mediated mechanism

This route seems to play an important role in  $NO$  formation in lean combustion and low temperatures, being triggered by the recombination of  $O$  atoms with  $N_2$ , generating  $N_2O$  mainly through the Reaction 6:



For lean conditions, the  $N_2O$  can be oxidize into  $NO$  or be reduced to  $N_2$ :



For rich stoichiometric conditions, the  $N_2O$  is mainly reduced into  $N_2$ :



From the last reactions, it is concluded that this trajectory becomes important under conditions of a high-pressure environment and excess air, due to the presence of third body reactions,  $M$ , being also enriched by the super equilibrium of atoms of  $O$  (Martins and Ferreira, 2010).

### 2.1.4 $NNH$ mechanism

This is the most recent route of  $NO$  formation found (Purohit *et al.*, 2021). The formation of  $NO$  in high temperatures through the  $NNH$  was proposed by Bozzelli and Deant (1995). This route for  $NO$  formation involves the Reaction 12:



The  $NNH$  reacts with oxygen atoms, forming  $HNNO^*$  that dissociates into  $NH + NO$  (Bozzelli and Deant, 1995). This route is related to be important in the  $NO_X$  formation in gas operating turbines and for long-chain hydrocarbon fuels (Bozzelli and Deant, 1995; Klippenstein *et al.*, 2011; Purohit *et al.*, 2021).

### 2.1.5 Nitrogen from the fuel

Nitrogen compounds present in the fuel, suffer rapid vaporization when entering the combustion chamber (when referring to liquid fuels). The production of atoms of nitrogen in the flame front on the fuel  $NO$  mechanism requires much less energy than the formation of nitrogen atoms via  $N_2 + O$  (Martins and Ferreira, 2010). According to Bowman (1973), the rate of  $NO$  formation via nitrogen-containing compounds (other than thermal  $NO$ ) occurs on a comparable time scale to those of combustion reactions.

## 2.2 Detailed kinetics models available in the literature

The chemical kinetics mechanisms are a set of chemical reactions that describes the kinetics evolution of chemical species, step by step, along the combustion process (Cancino, 2009). These mechanisms can be detailed, skeletal, or global models. As long as in this paper the  $NO_X$  formation is assessed, the mechanisms that are going to be presented, are those that consider this problem. Capriolo *et al.* (2021) proposed a mechanism for the combustion of  $C_3$  alcohols, consisting

of 203 species and 2295 reactions, based on the mechanism proposed by Capriolo and Konnov (2020). The mechanism was tested for well-stirred and flow reactors, flame structure, and ignition delay times, satisfactorily reproducing the experimental values. Ranzi *et al.* (2012) developed a comprehensive detailed kinetics model built hierarchically from small hydrocarbons ( $CH_4$ ) to heavy hydrocarbons (C-atoms  $\sim 16$ ), this model allows 483 chemical species among 19340 elementary reactions including the  $NO_X$  kinetics. In this work, two detailed kinetics models are used for numerical assessment of  $NO_X$  formation, mainly in the post-flame region. Table 1 list the main characteristics of that models.

Table 1: Detailed kinetics models for  $NO_X$  numerical assessment in this work

	A.KONNOV's DKM	POLIMIv1214NOXTot
Elements	6	6
Species	201	483
Reactions	2300	19340
Reference	Capriolo <i>et al.</i> (2021)	Ranzi <i>et al.</i> (2012)

### 3. METHODS

There is a lack of studies concerning the  $NO$  formation and consumption from propyl alcohol fuels. In this sense, the most recent work in the literature is the paper from Capriolo *et al.* (2021), where the authors proposed a kinetics mechanism for  $n$ -propanol and  $i$ -propanol combustion, and also presented new experimental data on  $NO$  formation in  $C_3$  alcohols/air flames. In addition, the POLIMI mechanism, (Metcalfe *et al.*, 2013; Pelucchi *et al.*, 2017; Song *et al.*, 2019) was compared to Capriolo's mechanism and the experimental data produced. In the work of Capriolo *et al.* (2021)  $NO$  and laminar burning velocity measurements in the post-flame region are made, and this experimental data is used in the present work to assess the performance of the kinetics models analyzed, see Table 1 for mechanism's details. Laminar flame speed simulations (burner stabilized flat flame reactor) were performed in order to numerically assess the kinetics model's performance.

All the numerical simulations in this work were performed with an in-house Python 3.6.13 script using the Cantera 2.4.0 toolkit. Cantera is an open-source suite of tools for solve problems involving chemical kinetics, thermodynamics, and transport processes. Inside the toolkit there are pre-defined functions, applied to solve the combustion problem applied to reactors, flames and chemical equilibrium<sup>1</sup>. The simulations were performed on a workstation with an Intel Core i7-7700 processor with 3.60 GHz and 16GB of memory RAM.

Aiming to comprehend how the radiative and diffusive effects affect the solution of the adiabatic, one-dimensional free flame<sup>2</sup>, it was analyzed for the combustion of  $n$ -propanol,  $C_3H_7OH$ , and  $i$ -propanol,  $(CH_3)_2CHOH$ , at an initial pressure of 1 atm and temperature of 373 K, with an equivalence ratio of 0.7-1.5. The refine criteria are: ratio of 3, the slope of 0.1, and curve of 0.1, relating to the transport model, the multicomponent model was used. Regarding the diffusive mass fluxes, Soret effect, and radiative heat transfer, the influence of these effects was investigated. In this analysis two cases were simulated, one whit the radiative and diffusive effects enabled, and another with the effects disabled. The analysis was done for the three mechanisms outlined in Table 1. As well, the reactions considered in the detailed kinetics modes were checked, in order to verify if all the  $NO_X$  formation routes are considered, addressing to comprehend the differences in the results obtained in the three mechanisms. The Capriolo *et al.* (2021) mechanism took an average simulation time of 3 hours and 40 minutes, while Ranzi *et al.* (2012) mechanism took 87 hours.

### 4. RESULTS AND DISCUSSION

The results obtained for the combustion of the alcohols are presented in this section, starting with a comparison between the predictions made by the kinetic mechanisms and the experimental data, aiming to verify the accuracy of the outlined mechanisms. The comparisons are in terms of the  $NO$  mole fraction prediction in the post-flame region, the laminar burning velocity (LBV), and the temperature at 10 mm above the burner.

#### 4.1 $NO$ mole fraction

The  $NO$  mole fraction in the post-flame region is presented in Figure 1 for an equivalence ration between 0.7-1.5, where, the result for  $n$ -propanol is shown in Figure 1(a), and for  $i$ -propanol in Figure 1(b). In Figure 1 the experimental data is presented along with the numerical solution results obtained with the two mechanisms, where each mechanism is presented twice, firstly with the “+” sign, indicating that the thermal diffusion and radiative heat losses were leaving into account for the calculations, and, secondly, without the “+” sign, denoting that the thermal diffusion and the radiative

<sup>1</sup>Additional information about Cantera can be found at Cantera website.

<sup>2</sup>The description of this function can be found in the documentation available at Cantera website.

heat losses were not enabled. It is important to highlight that this pattern is used throughout the whole paper.

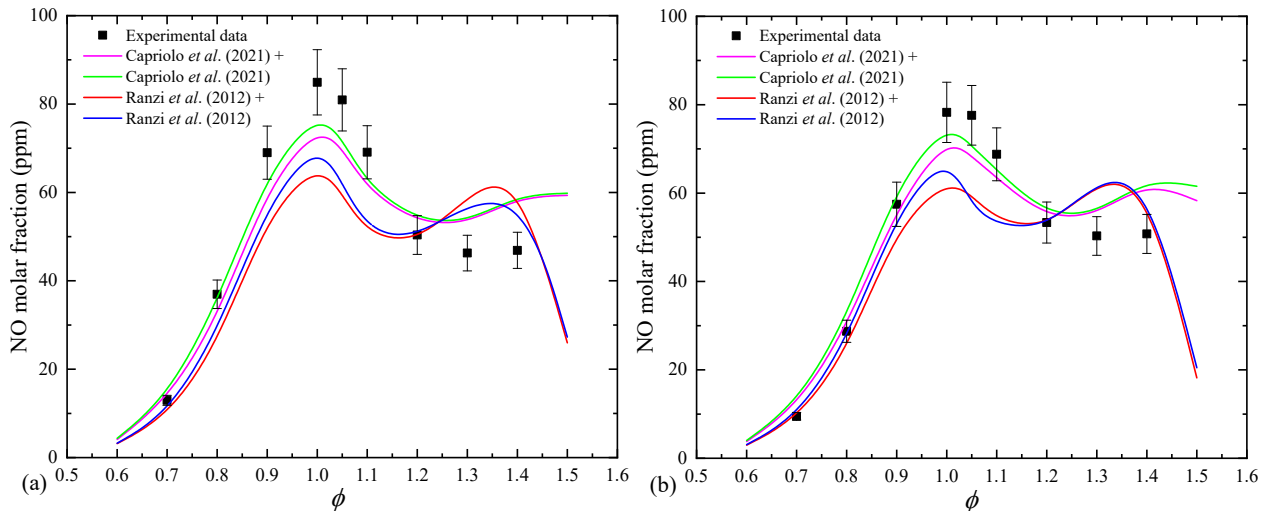


Figure 1: *NO* predictions using the detailed kinetics model from Capriolo *et al.* (2021) and Ranzi *et al.* (2012) for laminar flat flame of (a) *n*-propanol and (b) *i*-propanol. Experimental data from Capriolo *et al.* (2021). Unburned gas conditions:  $T = 323$  K and  $p = 1$  atm.

In Figure 1 the experimental data is represented by the black squares, along with its respective errors, Capriolo *et al.* (2021) mechanism with diffusion and radiation enabled is symbolized by the solid pink line, the Capriolo *et al.* (2021) mechanism without diffusion and radiation is the solid green line. The solid red line is related to Ranzi *et al.* (2012) mechanism with diffusion and radiation activated, while the solid blue line depicts the Ranzi *et al.* (2012) mechanism without diffusion and radiation in the calculations.

Concerning to *n*-propanol, in Figure 1(a) it is verified that the behavior of both mechanisms are very similar to the experimental data, for equivalence ratios lower than 1.2, for higher ratios the mechanisms no longer show similar results, with Capriolo *et al.* (2021) keeping a smooth increase in the *NO* mole fraction prediction, while Ranzi *et al.* (2012) presents a slight increase followed by a drastic decrease of the mole fraction. It is important to point out, that, the latter equivalence ratios are beyond above the stoichiometric ratio.

For small equivalence ratio, below 0.7, all the data has the same behavior, however, for the equivalence ratio between 0.9 and 1.1, the simulations without the radiative and diffusive effects showed higher *NO* molar fractions in comparison to the case where the effects are enabled. Also for the stoichiometric ratio, the *NO* molar fraction obtained without the effects for *i*-propanol and Capriolo *et al.* (2021) is inside the interval of the uncertainties of the experimental data. For the equivalence ratio higher than 1.2 there were no significant differences between the simulations. Regarding the found difference, despite it is small, of the order of 3-5 ppm, concerning environmental standards, this difference may be decisive for the acceptance or rejection of a given combustion process.

Another substantial information present in Figure 1(a) is that both mechanisms sub predicted the real *NO* mole fraction in the post flame region, with Capriolo *et al.* (2021) mechanism performing a better agreement with the experimental data, however, both mechanisms, however, both mechanisms were not able to correctly reproduce the behavior close to the stoichiometric ratio, with the Capriolo *et al.* (2021) mechanism having a result a little closer to the experimental data, compared to the Ranzi *et al.* (2012) mechanism.

Regarding the influence of the thermal diffusion and the radiative heat losses in the solution, it is observed, for Capriolo *et al.* (2021) mechanism, that, when these phenomena were left into account the *NO* mole prediction is closer to the experimental data, with a similar behavior occurring for Ranzi *et al.* (2012) mechanism (for equivalence ratio lower than 1.2). Ultimately, regarding the *NO* mole prediction, for *n*-propanol, it is possible to conclude that Capriolo *et al.* (2021) mechanism presents the better agreement with the experimental data, even though, it is clear that exists a significant difference between the prediction and the experimental values.

Concerning the combustion of *i*-propanol, the general behavior of the mechanisms is almost the same. Over again, when the thermal diffusion and the radiative heat losses were not accounted into the solution, the result came closer to the experimental data presented, also, Capriolo *et al.* (2021) mechanism presented a better agreement with the experimental data compared to Ranzi *et al.* (2012) mechanism.

## 4.2 Laminar burning velocity

Another important combustion parameter refers to the laminar burning velocity (LBV), which is depicted in Figure 2. The experimental data is symbolized by the black squares, along with its respective errors, Capriolo *et al.* (2021) mech-

anism with diffusion and radiation enabled is represented by the solid pink line, the Capriolo *et al.* (2021) mechanism without diffusion and radiation is represented by the solid green line. The solid red line represents Ranzi *et al.* (2012) mechanism with diffusion and radiation activated, while the solid blue line is related to the Ranzi *et al.* (2012) mechanism without diffusion and radiation in the calculations.

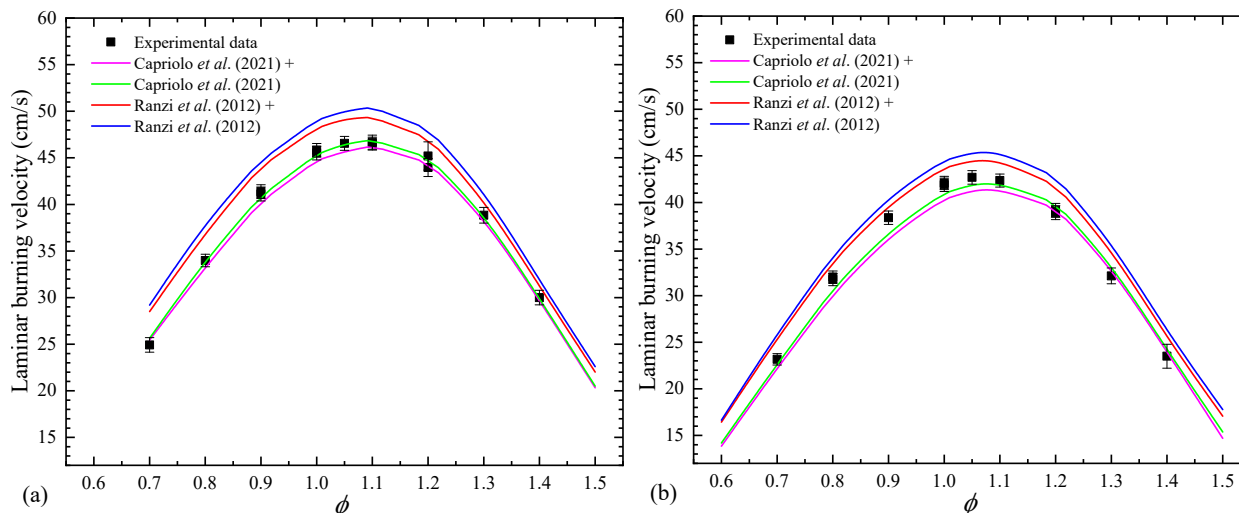


Figure 2: Laminar burning velocity predictions using the detailed kinetics model from Capriolo *et al.* (2021) and Ranzi *et al.* (2012) for laminar flat flame of (a) *n*-propanol and (b) *i*-propanol. Experimental data from Capriolo *et al.* (2021). Unburned gas conditions:  $T = 323$  K and  $p = 1$  atm.

Analyzing Figure 2 it can be noted that, for all the studied equivalence ratios, and both fuels, the Ranzi *et al.* (2012) mechanism overestimates the laminar burning velocity in comparison with both the Capriolo *et al.* (2021) mechanism and the experimental data, with this overestimation taking place far beyond the experimental data errors.

For all cases presented in Figure 2(a), we see that for Capriolo *et al.* (2021) mechanism the difference between the predicted laminar flame velocities is very small, being close to the value found experimentally. Based on the result in Figure 2(a), it can be concluded that for this variable, the consideration of thermal radiative and diffusive phenomena is almost indifferent, once that for both cases, almost all the predicted results remained inside the acceptable values, namely the errors of the experimental data.

Concerning to the *i*-propanol, its LBV is presented in Figure 2(b). Firstly, it is important to highlight that the LBV is lower in comparison with the values obtained for *n*-propanol in the same range of equivalence ratio. Secondly, the general behavior of the mechanisms observed for the mechanisms in the combustion of *n*-propanol is shown, that is, the Ranzi *et al.* (2012) mechanism presented higher results compared to Capriolo *et al.* (2021) mechanism, and, when the thermal diffusion and the radiative heat losses were not enabled, the LBV values were higher.

Since the method used by (Capriolo *et al.*, 2021) to measure the concentration of species in the post-flame region has high reliability, the doubt regarding the results lies with the kinetic mechanisms and the method of calculation of thermal radiative and diffusive phenomena for Cantera. Since the radiative heat exchange and Soret effect models are important in the combustion solution, these effects are well implemented in Cantera. But despite the above, in the present work, a detailed analysis of the referred model was not carried out so that it would not be possible to accurately determine how the model is operating. Thus, this difference may be due to a flaw in the kinetic model or due to a calibration that is modifying the results in a way that is not understood.

### 4.3 Temperature at 10 mm above the burner

Some *NO* formation routes deeply depend on the temperature of the flame and the post-flame products to be activated. In this sense, the temperature 10 mm above the burner is compared for both fuels and both mechanisms, and are presented in Figure 3.

For both fuels and mechanisms in Figure 3 it is clear that, when the radiative and thermal diffusive are not enabled, for all the equivalence ratio analyzed, the temperature is greater than the temperature when the effects were left into account in the calculations. These lower temperatures could be one of the reasons that explain the lower *NO* mole fraction and LBV prediction made by the kinetic mechanisms when the thermal losses related to the radiative effects were not enabled. Even though, it is comprehended that in terms of the *NO<sub>x</sub>* formation, this difference becomes more significant, showing that, through this perspective, the consideration of the diffusive and radiative effects is important.

The different temperatures developed by each mechanism could be one of the reasons for the difference in the *NO* mole fraction prediction, caused by different kinetic routes in the mechanisms. In this context, both mechanisms were

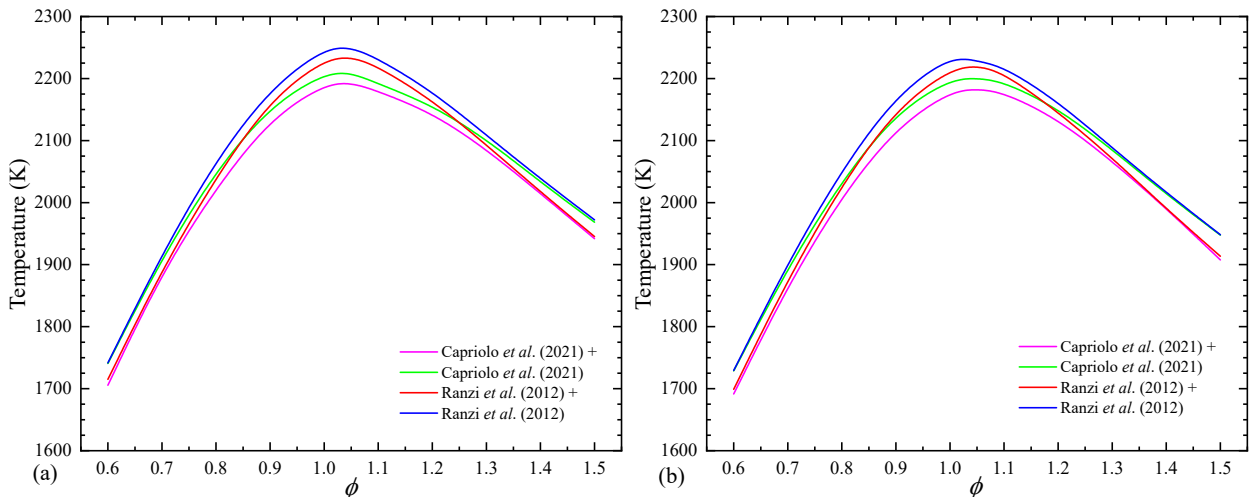


Figure 3: Temperature predictions using the detailed kinetics model from Capriolo *et al.* (2021) and Ranzi *et al.* (2012) for laminar flat flame of (a) *n*-propanol and (b) *i*-propanol. Unburned gas conditions:  $T = 323$  K and  $p = 1$  atm.

checked, being found that, all the  $NO_X$  formation routes are considered in both mechanisms. Nevertheless, the reactions rate constants in each mechanism are different substantially different, especially for the  $NNH$  mechanism, and  $N_2O$ -mediated mechanism for rich stoichiometric conditions.

Although, the full comprehension over which of the reactions, or the routes, influences more the predictions presented above, a sensitivity analysis must be done. This analysis is going to identify the most influencing reactions, allowing the upgrade of the Arrhenius parameters in the kinetic mechanisms.

#### 4.4 $NO_2$ mole fraction

Complementary to what was discussed in the previous sections, to fully observe the behavior of  $NO_X$ , it is presented in Figure 4 the  $NO_2$  mole fraction in  $ppb^3$ . Since the fuels have similar combustion characteristics, and the mechanisms presented close results, to facilitate the visualization and comparison of the results, in Figure 4(a) the  $NO_2$  mole fraction prediction for *n*-propanol using the Capriolo *et al.* (2021) mechanism is presented, and in Figure 4(b) the results for *i*-propanol using the Ranzi *et al.* (2012) mechanism. This exhibition allows the visualization of the difference that the diffusive and radiative effects cause in the solution. In both figures the legend with “+” sign is related to the case where the diffusive and radiative effects are enabled, and without the “+” sign where the effects are disabled.

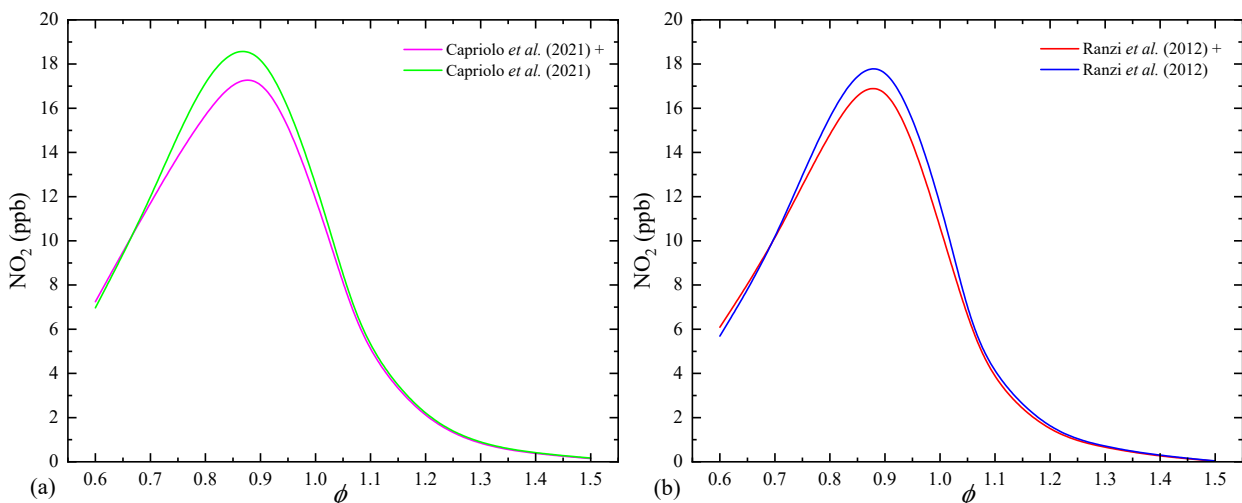


Figure 4:  $NO_2$  predictions using the detailed kinetics model from (a) Capriolo *et al.* (2021) and (b) Ranzi *et al.* (2012) for laminar flat flame. Unburned gas conditions:  $T = 323$  K and  $p = 1$  atm.

Analyzing Figure 4 it is clear that the difference between the molar fractions of  $NO_2$  in the two cases is very small, anyway, despite the small difference, depending on the application and the environmental standards, this difference may

<sup>3</sup>parts per billion.

be very significant.

## 5. CONCLUSION

The post-flame region experimental data is a very important tool, once it allows the verification of the accuracy of the kinetic mechanisms. In this sense, it is important to highlight that each kinetic mechanism could be tuned to better agree with a specific variable. Hereupon, it was verified that concerning the *NO* mole prediction, the mechanisms better predicted for the combustion of *i*-propanol for equivalence ratios lower than 0.9. For higher equivalence ratios the predicted values did not agree too well as for lower equivalence ratios. In conclusion, the Capriolo *et al.* (2021) mechanism made a better than the Ranzi *et al.* (2012) mechanism. Regarding the *NO* mole fraction for the combustion of *n*-propanol the predictions were less accurate than those for *i*-propanol, with the equivalence ratio lower than 0.8 being the best agreement made by them.

The laminar burning velocity for the combustion of *n*-propanol, Capriolo *et al.* (2021) mechanism performed better, for the full equivalence ratio range studied. For *i*-propanol, the results did not match so well the experimental data, although, the Capriolo *et al.* (2021) mechanism did a better prediction than Ranzi *et al.* (2012) mechanism, which, for both fuels, made an over prediction.

The temperature and the *NO*<sub>2</sub> mole prediction followed the same behaviors presented for *NO* mole fraction and LBV, once again Ranzi *et al.* (2012) mechanism made a prediction higher than Capriolo *et al.* (2021) mechanism. As is known, the temperature highly influences the *NO* formation, and, the higher temperature presented by Ranzi *et al.* (2012) mechanism could be one of the main causes of the higher *NO* mole fraction prediction and laminar burning velocity.

Relating to the *NO*<sub>x</sub> formation routes, both mechanisms consider the known routes presented in this paper, except the nitrogen from the fuel route, which makes sense, as long as the fuels used in this work are alcohols and do not have nitrogen in their chemical composition. Concerning the Arrhenius parameters used in the mechanisms, for the *NO*<sub>x</sub> reactions, there are some differences between Capriolo *et al.* (2021) and Ranzi *et al.* (2012), what could explain the different results obtained, even though, a sensibility analysis is required, to point out the most influencing reactions.

In relation to the effects of the thermal diffusive and radiative heat loss, knowing that heat exchange by radiation is a thermal loss, this reduced energy present in the flame modifies the kinetic mechanisms and that the reaction rates depend on the concentrations of the products, that are modified by the diffusive effects of the species occurring in the flame, it can be said that radiative thermal exchange and the Soret effect cannot be ignored, being important effects in the flame solution, mainly because they change the molar fractions of the products.

## 6. ACKNOWLEDGEMENTS

This study was financed in part by the Coordenação de Aperfeiçoamento de Pessoal de Nível Superior – Brasil (CAPES) – Finance Code 001. The fourth author thanks the financial support from Nacional Petroleum, Natural Gás and Biofuels Agency - ANP -, from Financier of Studies and Projects - FINEP - and the Ministry of Science, Technology and Innovation - MCTI through the ANP's Human Resources Program for the Oil and Gas Sector - PRH-ANP/MCTI.

## 7. REFERENCES

- Ali, G., Zhang, T., Wu, W. and Zhou, Y., 2020. "Effect of hydrogen addition on NO<sub>x</sub> formation mechanism and pathways in MILD combustion of H<sub>2</sub>-rich low calorific value fuels". *International Journal of Hydrogen Energy*, Vol. 45, No. 15, pp. 9200–9210. ISSN 03603199. doi:10.1016/j.ijhydene.2020.01.027. URL <https://doi.org/10.1016/j.ijhydene.2020.01.027>.
- Bowman, C.T., 1973. "Kinetics of nitric oxide formation in combustion processes". *Symposium (International) on Combustion*, Vol. 14, No. 1, pp. 729–738. ISSN 00820784. doi:10.1016/S0082-0784(73)80068-2.
- Bozzelli, J.W. and Deant, A.M., 1995. "O + NNH: A Possible New Route". *International Journal of Chemical Kinetics*, Vol. 27, pp. 1097–1109.
- Cancino, L., 2009. *Development and Application of Detailed Chemical Kinetics Mechanisms for Ethanol and Ethanol Containing Hydrocarbon Fuels*. Ph.D. thesis, Federal University of Santa Catarina, Florianópolis. URL <https://www.tede.ufsc.br/teses/PEMC1184-T.pdf>.
- Capriolo, G., Brackmann, C., Lubrano Lavadera, M., Methling, T. and Konnov, A.A., 2021. "An experimental and kinetic modeling study on nitric oxide formation in premixed C<sub>3</sub>alcohols flames". *Proceedings of the Combustion Institute*, Vol. 38, No. 1, pp. 805–812. ISSN 15407489. doi:10.1016/j.proci.2020.07.051. URL <https://doi.org/10.1016/j.proci.2020.07.051>.
- Capriolo, G. and Konnov, A.A., 2020. "Combustion of propanol isomers: Experimental and kinetic modeling study". *Combustion and Flame*, Vol. 218, pp. 189–204. ISSN 15562921. doi:10.1016/j.combustflame.2020.05.012.
- De Soete, G.G., 1975. "Overall reaction rates of NO and N<sub>2</sub> formation from fuel nitrogen". *Symposium (International) on Combustion*, Vol. 15, No. 1, pp. 1093–1102. ISSN 00820784. doi:10.1016/S0082-0784(75)80374-2.

- Han, X., Marco, L.L., Brackmann, C., Wang, Z., He, Y. and Konnov, A.A., 2021. “Experimental and kinetic modeling study of NO formation in premixed CH<sub>4</sub>+O<sub>2</sub>+N<sub>2</sub> flames”. *Combustion and Flame*, Vol. 223, pp. 349–360. ISSN 15562921. doi:10.1016/j.combustflame.2020.10.010. URL <https://doi.org/10.1016/j.combustflame.2020.10.010>.
- IEA, 2019. “World energy balances: An Overview”. ISSN 1098-6596. doi:10.1017/CBO9781107415324.004. URL <https://www.iea.org/reports/world-energy-balances-2019>.
- Klippenstein, S.J., Harding, L.B., Glarborg, P. and Miller, J.A., 2011. “The role of NNH in NO formation and control”. *Combustion and Flame*, Vol. 158, No. 4, pp. 774–789. ISSN 00102180. doi:10.1016/j.combustflame.2010.12.013. URL <http://dx.doi.org/10.1016/j.combustflame.2010.12.013>.
- Lubrano Lavadera, M., Brackmann, C., Capriolo, G., Methling, T. and Konnov, A.A., 2021. “Measurements of the laminar burning velocities and NO concentrations in neat and blended ethanol and n-heptane flames”. *Fuel*, Vol. 288, No. September 2020, p. 119585. ISSN 00162361. doi:10.1016/j.fuel.2020.119585. URL <https://doi.org/10.1016/j.fuel.2020.119585>.
- Maroa, S. and Inambao, F., 2020. *Biodiesel, Combustion, Performance and Emissions Characteristics*. ISBN 9783030511654. doi:10.1007/978-3-030-51166-1. URL <https://doi.org/10.1007/978-3-030-51166-1>.
- Martins, C.A. and Ferreira, M.A., 2010. “Considerações sobre a formação de nox na combustão”. In *VI Congresso Nacional de Engenharia Mecânica. Campina Grande–Paraíba, Brasil*.
- McCaffery, C., Zhu, H., Tang, T., Li, C., Karavalakis, G., Cao, S., Oshinuga, A., Burnette, A., Johnson, K.C. and Durbin, T.D., 2021. “Real-world NO<sub>x</sub> emissions from heavy-duty diesel, natural gas, and diesel hybrid electric vehicles of different vocations on California roadways”. *Science of the Total Environment*, Vol. 784, p. 147224. ISSN 18791026. doi:10.1016/j.scitotenv.2021.147224. URL <https://doi.org/10.1016/j.scitotenv.2021.147224>.
- Metcalfe, W.K., Burke, S.M., Ahmed, S.S. and Curran, H.J., 2013. “A hierarchical and comparative kinetic modeling study of C1 - C2 hydrocarbon and oxygenated fuels”. *International Journal of Chemical Kinetics*, Vol. 45, No. 10, pp. 638–675. ISSN 05388066. doi:10.1002/kin.20802.
- Orooji, Y., Javadi, M., Karimi-Maleh, H., Aghaie, A.Z., Shayan, K., Sanati, A.L. and Darabi, R., 2021. “Numerical and experimental investigation of natural gas injection effects on NO<sub>x</sub> reburning at the rotary cement kiln exhaust”. *Process Safety and Environmental Protection*, Vol. 151, pp. 290–298. ISSN 09575820. doi:10.1016/j.psep.2021.05.019. URL <https://doi.org/10.1016/j.psep.2021.05.019>.
- Pelucchi, M., Bissoli, M., Rizzo, C., Zhang, Y., Somers, K., Frassoldati, A., Curran, H. and Faravelli, T., 2017. “A Kinetic Modelling Study of Alcohols Operating Regimes in a HCCI Engine”. *SAE International Journal of Engines*, Vol. 10, No. 5, pp. 2354–2370. ISSN 19463944. doi:10.4271/2017-24-0077.
- Purohit, A.L., Nalbandyan, A., Malte, P.C. and Novosselov, I.V., 2021. “NNH mechanism in low-NO<sub>x</sub> hydrogen combustion: Experimental and numerical analysis of formation pathways”. *Fuel*, Vol. 292, No. September 2020, p. 120186. ISSN 00162361. doi:10.1016/j.fuel.2021.120186. URL <https://doi.org/10.1016/j.fuel.2021.120186>.
- Ranzi, E., Frassoldati, A., Grana, R., Cuoci, A., Faravelli, T., Kelley, A.P. and Law, C.K., 2012. “Hierarchical and comparative kinetic modeling of laminar flame speeds of hydrocarbon and oxygenated fuels”. *Progress in Energy and Combustion Science*, Vol. 38, pp. 468–501. ISSN 0360-1285. doi:10.1016/j.pecs.2012.03.004.
- Song, Y., Marrodán, L., Vin, N., Herbinet, O., Assaf, E., Fittschen, C., Stagni, A., Faravelli, T., Alzueta, M.U. and Battin-Leclerc, F., 2019. “The sensitizing effects of NO<sub>2</sub> and NO on methane low temperature oxidation in a jet stirred reactor”. *Proceedings of the Combustion Institute*, Vol. 37, No. 1, pp. 667–675. ISSN 15407489. doi:10.1016/j.proci.2018.06.115. URL <https://doi.org/10.1016/j.proci.2018.06.115>.
- Watson, G.M., Versailles, P. and Bergthorson, J.M., 2016. “NO formation in premixed flames of C1-C3 alkanes and alcohols”. *Combustion and Flame*, Vol. 169, pp. 242–260. ISSN 15562921. doi:10.1016/j.combustflame.2016.04.015.

## 8. RESPONSIBILITY NOTICE

The authors are solely responsible for the printed material included in this paper.